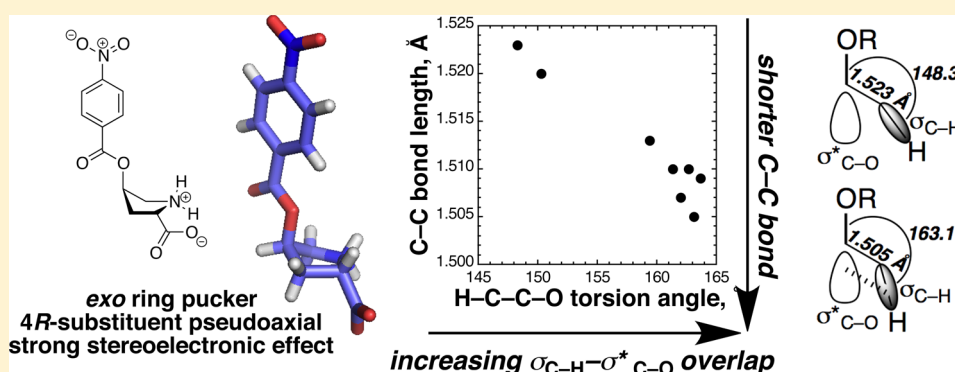


(2*S*,4*R*)-4-Hydroxyproline(4-nitrobenzoate): Strong Induction of Stereoelectronic Effects via a Readily Synthesized Proline Derivative. Crystallographic Observation of a Correlation between Torsion Angle and Bond Length in a Hyperconjugative Interaction

Anil K. Pandey, Glenn P. A. Yap,* and Neal J. Zondlo*

Department of Chemistry and Biochemistry, University of Delaware, Newark, Delaware 19716, United States

S Supporting Information



ABSTRACT: (2*S*,4*R*)-4-Hydroxyproline(4-nitrobenzoate) was synthesized. The crystal structure revealed an exo ring pucker, with the nitrobenzoate pseudoaxial on the pyrrolidine envelope and antiperiplanar to C^β and C^δ C–H bonds. The unit cell exhibited variation in C^δ –H/ C^γ –O and C^β –H/ C^γ –O torsion angles, with a 15° increase in torsion angle (148° to 163°) observed to result in a 0.018 Å decrease in C^δ –H/ C^γ –O bond length, consistent with favorable $\sigma_{C-H} \rightarrow \sigma^*_{C-O}$ hyperconjugative interactions increasing with greater orbital overlap.

Proline is a unique amino acid due to its cyclic structure, which in proteins limits its conformation to the torsion angle $\phi = -65^\circ \pm 25^\circ$.^{1,2} 4-Substituted prolines, including the collagen constituent (2*S*,4*R*)-4-hydroxyproline, provide enhanced conformational control compared to proline via their relative preferences for the C^γ -exo versus C^γ -endo pyrrolidine ring puckers.^{3,4} In (2*S*,4*R*)-4-hydroxyproline, the pyrrolidine ring preferentially adopts an exo ring pucker, which in general leads to a greater preference for more compact conformations of proline and for a trans amide bond (Figure 1). Because proline side-chain conformation couples to the protein main chain, 4-substituted prolines can allow selective control of local peptide and protein structure and protein stability.^{3,5–18} Because of both conformational restriction of proline and the ability to readily incorporate additional functionality into proline amino acids using the hydroxyl group of the inexpensive amino acid (2*S*,4*R*)-4-hydroxyproline as a reactive handle, 4-substituted prolines have been widely employed in medicinal chemistry and in peptide and protein design.

In addition, proline and proline-derived molecules have recently emerged as effective catalysts for a series of carbonyl addition reactions, including aldol, Michael, and Mannich reactions.^{19–27} The incorporation of groups that can stabilize the structure of proline-based catalysts can substantially

modulate both reaction rate and stereoselectivity.^{21–23,25–27} For example, Chandler and List demonstrated in transannular intramolecular aldol reactions that (2*S*,4*R*)-4-fluoroproline exhibited substantially greater enantioselectivity and reaction rate than either (2*S*)-proline or the (2*S*,4*S*)-4-fluoroproline diastereomer and applied (2*S*,4*R*)-4-fluoroproline as a catalyst in the asymmetric total synthesis of (+)-hirsutene.²⁸

We have investigated the incorporation of 4-substituted prolines into peptides and miniproteins to control structure and function.^{9–11} In that work, we found that the nitrobenzoate of (4*R*)-hydroxyproline induced a particular conformation restriction (Figure 1, Table 1) that was greater than that of (4*R*)-hydroxyproline and similar to that of (4*R*)-fluoroproline. In the trp cage miniprotein, replacement of proline 12 with the 4-nitrobenzoate ester of (4*R*)-hydroxyproline resulted in a 13°C increase in thermal stability compared to proline and a 10°C increase in thermal stability compared to (4*R*)-hydroxyproline.¹⁰ Within model Ac-TYProxN-NH₂ tetrapeptides (Prox = proline derivative), the proline derivative that most favored the trans amide bond, which is usually associated with exo ring pucker preference, was the 4-nitrobenzoate of (4*R*)-hydrox-

Received: February 14, 2014

Published: April 10, 2014

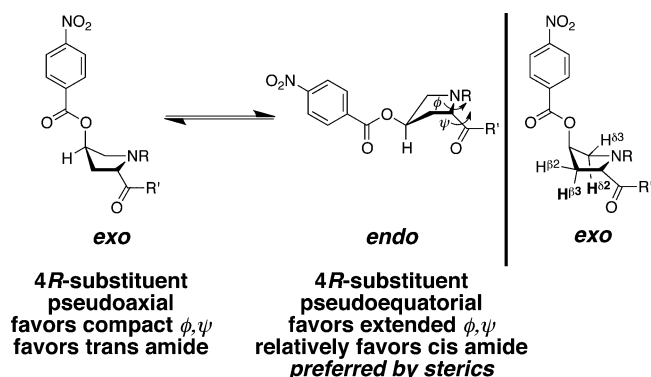


Figure 1. Left: (2*S*,4*R*)-4-hydroxyproline(4-nitrobenzoate) *exo* and *endo* ring pucker and the conformational preferences observed for proline residues with these ring pucker.^{6–8,11,18} Right: nomenclature of proline H^β and H^δ hydrogens, with hydrogens capable of engaging in hyperconjugative interactions (as the σ of $C^\beta-H^\beta$ or $C^\delta-H^\delta$ bonds), via overlap with the σ^* of the C' -nitrobenzoate, indicated in bold.

Table 1. NMR-Derived Data from Peptides with Proline and 4*R*-Substituted Prolines^a

Ac-TYXN-NH ₂ , X =	$K_{\text{trans/cis}}$	ΔG (kcal mol ^{−1})	$\Delta\Delta G$ (kcal mol ^{−1})	ref
Hyp(4-NO ₂ -Bz)	8.2	−1.25	−0.66	10, 11
Flp	7.0	−1.15	−0.56	9, 11
Hyp	5.6	−1.02	−0.43	9, 11
Pro	2.7	−0.59	0.00	9, 11

^a $\Delta G_{\text{trans/cis}} = -RT \ln K_{\text{trans/cis}}$. $\Delta\Delta G_{\text{trans/cis}} = \Delta G_{\text{trans/cis}}$ (peptide with proline derivative) − $\Delta G_{\text{trans/cis}}$ (peptide with proline), which indicates the magnitude of the structural effect. Experiments were conducted in 90% H₂O/10% D₂O with 5 mM phosphate buffer pH 4 and 25 mM NaCl. Hyp(4-NO₂-Bz): the 4-nitrobenzoate ester of (2*S*,4*R*)-4-hydroxyproline; Flp: (2*S*,4*R*)-4-fluoroproline; Hyp: (2*S*,4*R*)-4-hydroxyproline; Pro: 2*S*-proline.

proline.^{10,11} Overall comparison of the effects of substituents on amide cis–trans isomerism ($K_{\text{trans/cis}}$), via quantification of the effects on $K_{\text{trans/cis}}$ in the 4*R* versus 4*S* diastereomers of a substituent, revealed a total of 0.90 kcal/mol modulation of $\Delta\Delta G_{\text{trans/cis}}$ in Ac-TYProxN-NH₂ peptides and 0.82 kcal/mol in Ac-TAProxN-NH₂ peptides for the 4-nitrobenzoates of 4-hydroxyproline, compared to 0.91 and 0.87 kcal/mol for fluorine substitution (i.e., 4-fluoroprolines) and 0.43 and 0.56 kcal/mol for hydroxyl substitution (i.e., 4-hydroxyprolines). Moreover, analysis of the NMR spectra of these peptides revealed greater overall amide chemical shift dispersion and greater dispersion of proline ring hydrogen chemical shifts for (4*R*)-hydroxyproline(4-nitrobenzoate) than for 4*R*-hydroxyproline or proline (Figures S1, S2, Supporting Information), indicating greater conformational restriction for nitrobenzoate substitution than hydroxyl substitution.¹¹ Collectively, these

data are consistent with the nitrobenzoate inducing strong stereoelectronic effects that are comparable to those of fluorine and greater than those of hydroxyl. However, in the absence of crystallographic data, it is possible that the effects observed for the 4-nitrobenzoate of (4*R*)-hydroxyproline could be due to unforeseen structural effects of the nitrobenzoate. Therefore, we sought independent determination of the effects of the hydroxyproline nitrobenzoate on proline structure.

While the (4*S*)-hydroxyproline nitrobenzoates are common intermediates in the synthesis of proline derivatives,^{29,30} via Mitsunobu reaction of (4*R*)-hydroxyproline with 4-nitrobenzoic acid, the 4*R* derivative had never previously been described. In our previous work, we demonstrated the facile incorporation of this amino acid within fully synthesized peptides using a method termed proline editing, in which a selectively deprotected (4*R*)-hydroxyproline-containing peptide was converted to contain one of over 120 diverse proline amino acids in high yield via practical chemistry on the solid phase.^{9–11}

The peptides synthesized via proline editing were readily analyzed by NMR spectroscopy. However, these peptides were not amenable to crystallization. Therefore, we embarked upon the synthesis of the free amino acid, which could potentially be crystalline. The nitrobenzoate was readily synthesized (Scheme 1) by esterification of the hydroxyl group on the methyl ester of Boc-(2*S*,4*R*)-4-hydroxyproline, a compound that is commercially available or synthesized in 1 step from inexpensive Boc-(2*S*,4*R*)-4-hydroxyproline. This product was subjected to acidic deprotection, which generated the crystalline free amino acid.

X-ray diffraction revealed the structure of the zwitterionic form of this amino acid (Figures 2–4, Table 2), with four

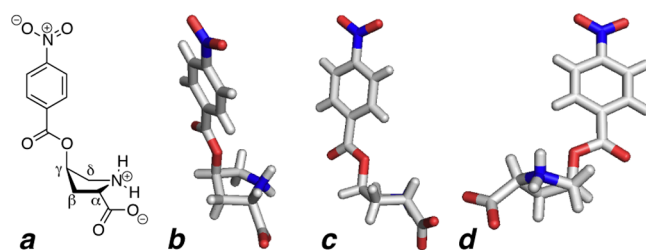
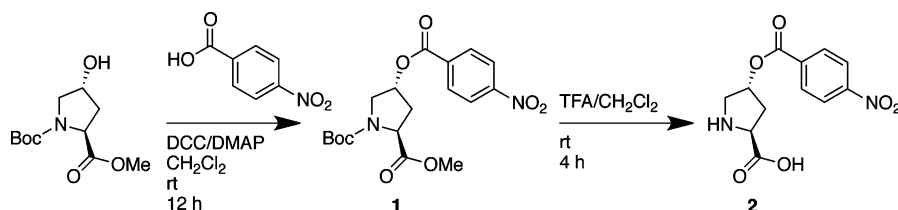


Figure 2. Crystallographically determined structure of one molecule of (2*S*,4*R*)-4-hydroxyproline(4-nitrobenzoate). (a,b) Overall molecular structure. (c) View with nonenvelope proline carbons in a plane perpendicular to the page, demonstrating the envelope pseudoaxial conformation of the nitrobenzoate. (d) View down the $C^\delta-C'$ bond, showing the antiperiplanar relationship of the $C^\delta-H^{\delta 2}$ bond and $C^\gamma-O$ bond and the gauche relationship of the $C^\gamma-O$ bond with the $C^\delta-N$ and $C^\beta-C^\alpha$ bonds. Entry (c) also shows the antiperiplanar relationship of the $C^\beta-H^{\beta 3}$ and $C^\gamma-O$ bonds. The ammonium hydrogens in the crystal are the deuterium isotope of hydrogen.

Scheme 1. Synthesis of (2*S*,4*R*)-4-Hydroxyproline(4-nitrobenzoate)



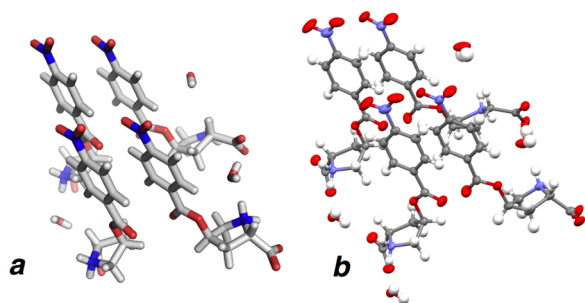


Figure 3. Crystallographic data of (2*S*,4*R*)-4-hydroxyproline(4-nitrobenzoate): (a) unit cell topology, with 4 molecules in the unit cell; (b) thermal ellipsoids (50% probability).

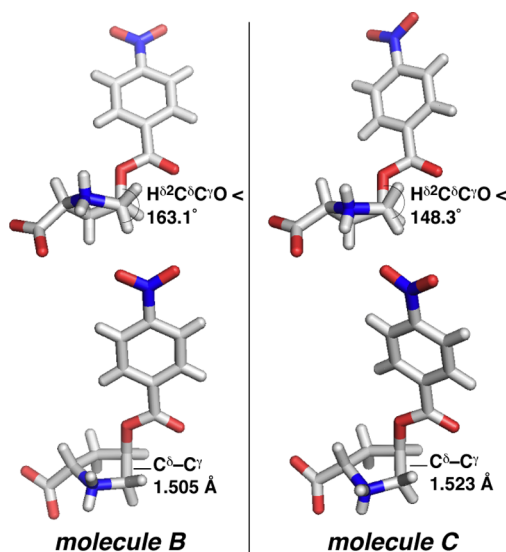


Figure 4. Comparison of two molecules in the unit cell exhibiting divergent $\text{H}^{\delta 2}\text{-C}^{\delta}\text{-C}^{\gamma}\text{-O}$ torsion angles (top) and $\text{C}^{\delta}\text{-C}^{\gamma}$ bond lengths (bottom).

symmetry-unique molecules in the asymmetric unit. The molecules pair such that two distinct hydrogen-bonded polymers are formed by water bridging an ammonium donor to two carboxylate acceptors (Figure S3, Supporting Information). The two polymers differ in the identity of the linking carboxylate. In polymer A, both carboxylate acceptors are from two symmetry equivalent molecules while in polymer B the acceptors are from two symmetry-unique molecules. Crystal packing resulted from a slip-stack alignment of ABA polymers with the aromatic groups in parallel-displaced planes 3.5 Å apart, which allowed favorable interactions between the positively and negatively charged components of the aromatic rings, similar to other cases displaying $\pi\text{-}\pi$ interactions.^{31,32}

The amino acid adopted a structure consistent with a strong stereoelectronic effect induced by the nitrobenzoate, as had been suggested by peptide NMR data. The proline ring adopted a $\text{C}^{\gamma}\text{-exo}$ ring pucker (Figure 2c), with the nitrobenzoate at the pseudoaxial position of the envelope of the pyrrolidine ring. This conformation is sterically unfavorable due to gauche interactions with the ring and due to the nitrobenzoate being on the concave (inward) face of the pyrrolidine envelope. The magnitude of this latter interaction is reduced by rotation of the $\text{C}^{\gamma}\text{-O}$ bond to place the nonconjugated oxygen lone pair into the envelope and the carbonyl away from the envelope. The plane of the aromatic ring is overall nearly orthogonal to the plane of the pyrrolidine ring, with the nitrobenzoate extending far above the proline ring. These data suggest that the observed strong conformational preferences of the hydroxyproline nitrobenzoate were probably not due to specific interactions of the aromatic nitrobenzoate group, but rather due to the electron-withdrawing nature of the nitrobenzoate group resulting in a strong preference for the *exo* ring pucker.

Closer analysis of the crystal structure indicates that (2*S*,4*R*)-4-hydroxyproline(4-nitrobenzoate) adopts a structure in the proline ring that is nearly identical to that of Ac-(2*S*,4*R*)-4-fluoroproline-OMe (Ac-Flp-OMe) (CSD code: RISDEC), which exhibits strong stereoelectronic effects due to the highly electron-withdrawing nature of fluorine.^{3,33} The $\text{C}^{\gamma}\text{-O}$ bond exhibits gauche relationships with both the $\text{C}^{\beta}\text{-C}^{\alpha}$ and $\text{C}^{\delta}\text{-N}$ bonds (Table 2), in opposition to the expectations of sterics. In contrast, the nitrobenzoate $\text{C}^{\gamma}\text{-O}$ bond is close to antiperiplanar with the $\text{C}^{\delta}\text{-H}^{\delta 2}$ (163.1° , 162.7° , 148.3° , and 163.7°) and $\text{C}^{\beta}\text{-H}^{\beta 3}$ (162.0° , 161.4° , 159.4° , and 150.3°) bonds. These results are consistent with a typical gauche effect and, in particular, are very similar to the gauche effect observed for (4*R*)-fluoroproline or (4*R*)-acetoxypoline.

Interestingly, the molecule with the largest deviation from an antiperiplanar arrangement between the $\text{C}^{\gamma}\text{-O}$ and $\text{C}^{\delta}\text{-H}^{\delta 2}$ bonds (148.3°) had a longer $\text{C}^{\gamma}\text{-C}^{\delta}$ bond (1.523 Å) than the other $\text{C}^{\gamma}\text{-C}^{\delta}$ bonds (1.505, 1.509, 1.510 Å), consistent with the expected contraction of the C-C bond due to hyperconjugation in the latter molecules (Figure 4, Table 2). Similarly, the molecule with the largest deviation from an antiperiplanar arrangement of the $\text{C}^{\gamma}\text{-O}$ and $\text{C}^{\beta}\text{-H}^{\beta 3}$ bonds (150.3°) had the longest $\text{C}^{\beta}\text{-C}^{\gamma}$ bond (1.520 Å, versus 1.507 Å (162.0°), 1.510 Å (161.4°), and 1.513 Å (159.4°)). Considering all potential hyperconjugative interactions with the nitrobenzoate, we observed a correlation between the C-H/C-O torsion angle and the bond lengths of those C-C bonds (Figure 5). These data suggest that the bond contraction observed was specifically due to favorable hyperconjugative interactions induced by the highly electron-withdrawing nitrobenzoate group.

Table 2. Torsion Angles (deg) and Bond Lengths (Å) for Bonds Associated with C^{γ} from Different Molecules in the Unit Cell^a

molecule	$\text{H}^{\delta 2}\text{-C}^{\delta}\text{-C}^{\gamma}\text{-O}$ (deg)	$\text{C}^{\delta}\text{-C}^{\gamma}$ (Å)	$\text{H}^{\beta 3}\text{-C}^{\beta}\text{-C}^{\gamma}\text{-O}$ (deg)	$\text{C}^{\beta}\text{-C}^{\gamma}$ (Å)	$\text{C}^{\gamma}\text{-O}$ (Å)	$\text{C}^{\alpha}\text{-C}^{\beta}\text{-C}^{\gamma}\text{-O}$ (deg)	$\text{N-C}^{\delta}\text{-C}^{\gamma}\text{-O}$ (deg)
A	162.7(3)	1.510(4)	161.4(3)	1.510(4)	1.459(4)	-79.1(3)	-78.0(3)
B	163.1(3)	1.505(4)	162.0(3)	1.507(4)	1.459(4)	-78.5(3)	-77.5(3)
C	148.3(3)	1.523(4)	159.4(3)	1.513(4)	1.453(4)	-81.3(3)	-92.1(3)
D	163.7(3)	1.509(5)	150.3(3)	1.520(5)	1.459(4)	-89.9(3)	-77.2(3)

^aNumbers in parentheses are the standard errors of the last digit. $\text{H}^{\delta 2}\text{-C}^{\delta}\text{-C}^{\gamma}\text{-O}$ torsion angles are negative in sign and are reported here as the absolute value of the torsion angle for comparison to $\text{H}^{\beta 3}\text{-C}^{\beta}\text{-C}^{\gamma}\text{-O}$.

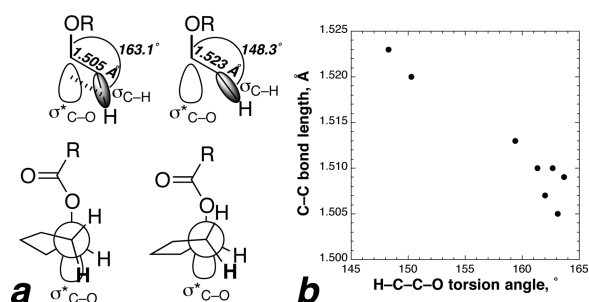


Figure 5. Association of torsion angle with orbital overlap and bond length. (a) Orbital overlap of $\sigma^*_{\text{C-O}}$ with the $\sigma_{\text{C-H}}$ orbital ($\text{C}^\delta\text{-H}^{\delta 2}$ bond) for the $\text{C}^\delta\text{-C}^\gamma$ bonds in molecule B (left) and molecule C (right). The larger torsion angle (left) exhibits better orbital overlap of the donor $\sigma_{\text{C-H}}$ with the acceptor $\sigma^*_{\text{C-O}}$ and a shorter C-C bond. (b) Comparison of C-C bond length as a function of H-C-C-O torsion angle across all $\text{C}^\beta\text{-C}^\gamma$ ($\text{H}^\beta\text{-C}^\beta\text{-C}^\gamma\text{-O}$) and $\text{C}^\delta\text{-C}^\gamma$ ($\text{H}^{\delta 2}\text{-C}^\delta\text{-C}^\gamma\text{-O}$) bonds in the unit cell.

We have described the synthesis of the amino acid (2*S*,4*R*)-4-hydroxyproline(4-nitrobenzoate). This amino acid had previously been incorporated within peptides via proline editing, with the nitrobenzoate observed to induce one of the largest stereoelectronic effects of 4-substituted prolines. Here, we demonstrate the facile solution-phase synthesis of this amino acid in two steps from commercially available starting materials. (2*S*,4*R*)-4-Hydroxyproline(4-nitrobenzoate) exhibits stereoelectronic effects similar to those of (2*S*,4*R*)-4-fluoroproline but may be synthesized without requiring double inversion at the C4 stereocenter of the common starting material (2*S*,4*R*)-4-hydroxyproline.^{34–36} Combined with our previous demonstration of the incorporation of this amino acid within a peptide during solid-phase peptide synthesis, (2*S*,4*R*)-4-hydroxyproline-(4-nitrobenzoate) represents the easiest entry to a 4*R*-substituted proline derivative with a greater conformational preference than Hyp.

The crystal structure of (2*S*,4*R*)-4-hydroxyproline(4-nitrobenzoate) confirmed data in peptides that the 4-nitrobenzoate of hydroxyproline induces a strong stereoelectronic effect, with a $\text{C}^\gamma\text{-exo}$ ring pucker observed. Interestingly, the four molecules in the unit cell did not exhibit identical geometries. In two of the molecules, a classical stereoelectronic effect was observed, with strong overlap (torsion angle 159.4°–163.7°) of one $\text{C}^\delta\text{-H}^\delta$ and one $\text{C}^\beta\text{-H}^\beta$ bond with the σ^* of the $\text{C}^\gamma\text{-O}$ bond. In the other two molecules, one of the bonds to C^γ exhibited this effect. However, the other C-C bond in these molecules ($\text{C}^\gamma\text{-C}^\delta$ in molecule C; $\text{C}^\gamma\text{-C}^\beta$ in molecule D) exhibited a significant deviation (torsion angle 148.3°–150.3°) from these torsion angles, resulting in worse overlap of that C-H σ with the C-O σ^* .^{32,37} The observation of a smaller H-C-C-O torsion angle was associated with a significantly longer C-C bond. These data provide direct evidence supporting stabilizing hyperconjugative interactions leading to a contraction of the C-C bond length, compared to molecules of identical composition in a slightly different conformation (13°–15° deviation in torsion angle) lacking this stabilizing interaction.

The association of a greater extent of hyperconjugation with a shorter bond length is well-known in studies on the anomeric effect in glycosides and acetals.^{38–40} In these cases, strong evidence of hyperconjugation is obtained via the observation of shorter O-C endo bonds on molecules with axial electron-withdrawing substituents compared to stereoisomers which have equatorial electron-withdrawing substituents (as well as

longer exo bonds to the axial substituent compared to the equatorial substituent) or alternatively due to shortened endo O-C bonds in a series of molecules with more electron-withdrawing axial substituents (and longer exo bonds to the most electron-withdrawing substituents). In both of these classes of examples, the highly compelling data supporting the importance of stereoelectronic effects are obtained by comparison between stereoisomers or among nonisomeric compounds. In addition, these examples all are conducted with axial substituents that allow near-perfect (~180°) antiperiplanar arrangements of the groups, and thus near-perfect orbital overlap of the donor and acceptor orbitals. In contrast, the complementary data herein are obtained within different crystallographically observed conformations of a single molecule. These data reveal C-C bond contraction, indicative of greater bond strength, due to increased orbital overlap as a function of torsion angle. These results are expected but are challenging to observe experimentally and more typical of the results found via calculations. The work herein thus provides direct experimental evidence supporting the fundamental concept that the extent of orbital overlap in a stereoelectronic effect correlates with strengthening of the hyperconjugative interaction.

EXPERIMENTAL SECTION

Synthesis and Characterization. (2*S*,4*R*)-1-*tert*-Butyl 2-Methyl 4-((4-Nitrobenzoyl)oxy)pyrrolidine-1,2-dicarboxylate (**1**). (2*S*,4*R*)-1-*tert*-Butyl 2-methyl 4-hydroxypyrrolidine-1,2-dicarboxylate (5.00 g, 20.4 mmol) was dissolved in anhydrous CH_2Cl_2 (200 mL) at room temperature under N_2 . To the solution were added 4-nitrobenzoic acid (3.41 g, 20.4 mmol) and dicyclohexylcarbodiimide (DCC) (5.06 g, 24.5 mmol). A catalytic amount of *N,N*-(dimethylamino)pyridine (DMAP) (125 mg, 1.0 mmol) was added to the reaction mixture, and the resulting mixture was stirred vigorously for 12 h. The white precipitate was filtered, and the solvent was removed in vacuo. The resulting crude oil was purified by silica gel column chromatography (0–2% $\text{CH}_3\text{OH}/\text{CH}_2\text{Cl}_2$ v/v) to yield compound **1** (6.1 g) as a colorless oil (76% yield). The NMR data represent the major rotational isomer (*trans*). The minor *cis* rotational isomer was distinctly observed for a few resonances: ^1H NMR (600 MHz, CDCl_3) δ 8.32–8.30 (d, J = 8.8 Hz, 2H), 8.20–8.18 (d, J = 8.7 Hz, 2H), 5.58–5.57 (m, 1H), 4.56–4.52 (t, J = 7.8 Hz, minor), 4.47–4.43 (t, J = 8.1 Hz, major) (sum of major and minor = 1H), 3.91–3.85 (m, 1H), 3.79 (s, minor), 3.78 (s, major) (sum of major and minor = 3H), 3.73–3.70 (m, 1H), 2.61–2.58 (m, 1H), 2.40–2.32 (m, 1H), 1.47 (s, minor), and 1.44 (s, major) (sum of major and minor = 9H); ^{13}C NMR (151 MHz, CDCl_3) δ 173.0, 164.4, 153.9, 151.1, 135.2, 131.2, 124.0, 81.2, 74.7, 74.0, 58.2, 52.7, 36.9, and 28.6; ESI MS: $[\text{M} + \text{Na}]^+$ calcd for $\text{C}_{18}\text{H}_{22}\text{N}_2\text{O}_8\text{Na}$ 417.1, found 417.0; HRMS (LIFT-TOF) m/z $[\text{M}]^+$ calcd for $\text{C}_{18}\text{H}_{22}\text{N}_2\text{O}_8$ 394.1376; fragments observed: $[\text{M} - \text{C}_7\text{H}_5\text{NO}_4]^+$ calcd for $\text{C}_{11}\text{H}_{17}\text{NO}_4$ 227.1158, found 227.1146 (loss of nitrobenzoate); $[\text{M} - \text{C}_7\text{H}_3\text{NO}_3]^+$ calcd for $\text{C}_{11}\text{H}_{19}\text{NO}_5$ 245.1263, found 245.1234 (loss of nitrobenzoyl) (major fragment); $[\text{M} - \text{C}_5\text{H}_8\text{O}_2]^+$ calcd for $\text{C}_{13}\text{H}_{14}\text{N}_2\text{O}_6$ 294.0852, found 294.0865 (loss of Boc) (second most prominent fragment).

(2*S*,4*R*)-4-((4-Nitrobenzoyl)oxy)pyrrolidine-2-carboxylic Acid (**2**). Compound **1** (3.4 g, 8.6 mmol) was dissolved in anhydrous CH_2Cl_2 (20 mL) under a nitrogen atmosphere. Trifluoroacetic acid (CF_3COOH) (20 mL) was added to the solution, and the resulting reaction mixture was stirred at room temperature for 6 h. The solvent was removed in vacuo. The crude oil thus obtained was washed with cold ether (3 \times 15 mL) to obtain compound **2** (1.8 g) as a white solid (74% yield): ^1H NMR (600 MHz, D_2O) δ 8.46–8.37 (d, J = 7.2 Hz, 2H), 8.34–8.28 (d, J = 7.1 Hz, 2H), 5.77 (m, 1H), 4.87–4.82 (m, 1H), 4.61–4.54 (m, 1H), 3.90–3.74 (m, 2H), 2.90–2.84 (m, 1H), and 2.68–2.64 (m, 1H); ^{13}C NMR (151 MHz, $\text{D}_2\text{O}/\text{DMSO}-d_6$ (9:1)) δ 171.2, 162.2, 153.1, 137.4, 133.9, 126.3, 76.8, 60.1, 55.8, 53.2, and 36.7;

HRMS (LIFDI-TOF) m/z $[M + H]^+$ calcd for $C_{12}H_{13}N_2O_6$ 281.0774, found 281.0763.

X-ray Crystallography. Crystals were obtained from the slow evaporation of a solution of approximately 10 mg of compound **2** in 500 μ L of D_2O (Table 3). The systematic absences in the diffraction

Table 3. Crystallographic Data and Refinement Details

empirical formula	$C_{12}H_{14}N_2O_7$
formula weight	298.25
T (K)	200(2)
wavelength (\AA)	0.710 73
crystal system, space group	monoclinic, $P2_1$
unit cell dimensions (\AA , $^\circ$)	$a = 12.8822(17)$ $\alpha = 90$ $b = 9.5928(13)$ $\beta = 103.587(2)$ $c = 22.444(3)$ $\gamma = 90$
volume (\AA^3)	2696.0(6)
Z , Z' , calcd density (g/cm^3)	8, 4, 1.470
absorption coefficient (mm^{-1})	0.123
$F(000)$	1248
crystal size (mm)	$0.442 \times 0.334 \times 0.140$
θ range for data collection	1.626 to 27.736 deg.
limiting indices	$-16 \leq h \leq 16$, $-12 \leq k \leq 12$, $-29 \leq l \leq 29$
reflns collected/unique	63686/12602 [$R(\text{int}) = 0.0474$]
completeness to $\theta = 25.242(^\circ)$	99.9
absorption correction	semiempirical from equivalents
max and min transmission	0.7456 and 0.7063
refinement method	full-matrix least-squares on F^2
data/restraints/parameters	12602/51/805
goodness-of-fit on F^2	1.011
final R indices [$I > 2\sigma(I)$]	$R = 0.0437$, $wR^2 = 0.0906$
R indices (all data)	$R = 0.0712$, $wR^2 = 0.1039$
absolute structure parameter	$-0.3(3)$
largest diff peak and hole ($e/\text{\AA}^3$)	0.286 and -0.192

data are consistent with $P2_1$ and $P2_1/m$. The noncentrosymmetric space group option is consistent with the enantiomerically resolved sample. The absolute structure parameter refined to nil indicating the true hand of the data had been determined⁴¹ consistent with known chiral centers. The data set was treated with multiscan absorption corrections.⁴² The structure was solved using direct methods and refined with full-matrix, least-squares procedures on F^2 . All non-hydrogen atoms were refined with anisotropic displacement parameters. Four symmetry unique molecules of the zwitterion and four water molecules of hydration were located in the asymmetric unit. The water and ammonium H atoms were located from the difference map and treated with X–H and H–H geometrical restraints. All other hydrogen atoms were treated as idealized contributions with geometrically calculated positions and with U_{iso} equal to 1.2, or 1.5 for methyl, U_{eq} of the attached atom. The methylene H atom torsion angles were derived from the refined C–C bond positions and assuming idealized tetrahedral sp^3 geometry. Atomic scattering factors are contained in the SHELXL 2013 program library.⁴³ Structural information has been deposited with the Cambridge Crystallographic Data Centre under deposition no. CCDC 986367.

■ ASSOCIATED CONTENT

■ Supporting Information

Additional crystallographic data, CIF file, and 1H and ^{13}C NMR spectra of **1** and **2**. This material is available free of charge via the Internet at <http://pubs.acs.org>.

■ AUTHOR INFORMATION

Corresponding Authors

*E-mail: gyap@udel.edu. Tel: +1-302-831-4441.

*E-mail: zondlo@udel.edu. Tel: +1-302-831-0197. Fax: +1-302-831-6335.

Notes

The authors declare no competing financial interest.

■ ACKNOWLEDGMENTS

We thank the NIH (GM93225 and RR17716) and the University of Delaware for funding.

■ REFERENCES

- (1) MacArthur, M. W.; Thornton, J. M. *J. Mol. Biol.* **1991**, *218*, 397–412.
- (2) Reiersen, H.; Rees, A. R. *Trends Biochem. Sci.* **2001**, *26*, 679–684.
- (3) Bretscher, L. E.; Jenkins, C. L.; Taylor, K. M.; DeRider, M. L.; Raines, R. T. *J. Am. Chem. Soc.* **2001**, *123*, 777–778.
- (4) Jenkins, C. L.; Raines, R. T. *Nat. Prod. Rep.* **2002**, *19*, 49–59.
- (5) Horng, J. C.; Raines, R. T. *Protein Sci.* **2006**, *15*, 74–83.
- (6) Shoulders, M. D.; Satyshur, K. A.; Forest, K. T.; Raines, R. T. *Proc. Natl. Acad. Sci. U.S.A.* **2010**, *107*, 559–564.
- (7) Lovell, S. C.; Word, J. M.; Richardson, J. S.; Richardson, D. C. *Proteins* **2000**, *40*, 389–408.
- (8) Ho, B. K.; Coutasias, E. A.; Seok, C.; Dill, K. A. *Protein Sci.* **2005**, *14*, 1011–1018.
- (9) Thomas, K. M.; Naduthambi, D.; Triiya, G.; Zondlo, N. J. *Org. Lett.* **2005**, *7*, 2397–2400.
- (10) Naduthambi, D.; Zondlo, N. J. *J. Am. Chem. Soc.* **2006**, *128*, 12430–12431.
- (11) Pandey, A. K.; Naduthambi, D.; Thomas, K. M.; Zondlo, N. J. *J. Am. Chem. Soc.* **2013**, *135*, 4333–4363.
- (12) Renner, C.; Alefelder, S.; Bae, J. H.; Budisa, N.; Huber, R.; Moroder, L. *Angew. Chem., Int. Ed.* **2001**, *40*, 923–925.
- (13) Kim, W.; McMillan, R. A.; Snyder, J. P.; Conticello, V. P. *J. Am. Chem. Soc.* **2005**, *127*, 18121–18132.
- (14) Kim, W.; Hardcastle, K. L.; Conticello, V. P. *Angew. Chem., Int. Ed.* **2006**, *45*, 8141–8145.
- (15) Holzberger, B.; Marx, A. *J. Am. Chem. Soc.* **2010**, *132*, 15708–15713.
- (16) Crespo, M. D.; Rubini, M. *PLoS One* **2011**, *6*, e19425.
- (17) Sonntag, L. S.; Schweizer, S.; Ochsenfeld, C.; Wennemers, H. *J. Am. Chem. Soc.* **2006**, *128*, 14697–14703.
- (18) For an example of an endo ring pucker leading to a stronger preference for a trans amide bond, due to an intramolecular hydrogen bond, see: Kuemin, M.; Nagel, Y. A.; Schweizer, S.; Monnard, F. W.; Ochsenfeld, C.; Wennemers, H. *Angew. Chem., Int. Ed.* **2010**, *49*, 6324–6327.
- (19) List, B.; Lerner, R. A.; Barbas, C. F. *J. Am. Chem. Soc.* **2000**, *122*, 2395–2396.
- (20) List, B. *Tetrahedron* **2002**, *58*, 5573–5590.
- (21) Cheong, P. H.-Y.; Houk, K. N.; Warrier, J. S.; Hanessian, S. *Adv. Synth. Catal.* **2004**, *346*, 1111–1115.
- (22) Krattiger, P.; Kovasy, R.; Revell, J. D.; Ivan, S.; Wennemers, H. *Org. Lett.* **2005**, *7*, 1101–1103.
- (23) Bock, D. A.; Lehmann, C. W.; List, B. *Proc. Natl. Acad. Sci. U.S.A.* **2010**, *107*, 20636–20641.
- (24) Nielsen, M.; Worgull, D.; Zweifel, T.; Gschwend, B.; Bertelsen, S.; Jørgensen, K. A. *Chem. Commun.* **2011**, *47*, 632–649.
- (25) Zhao, Q.; Lam, Y.-h.; Kheirabadi, M.; Xu, C.; Houk, K. N.; Schafmeister, C. E. *J. Org. Chem.* **2012**, *77*, 4784–4792.
- (26) Albrecht, L.; Jiang, H.; Jørgensen, K. A. *Chem.—Eur. J.* **2014**, *20*, 358–368.
- (27) Zimmer, L. E.; Sparr, C.; Gilmour, R. *Angew. Chem., Int. Ed.* **2011**, *50*, 11860–11871.
- (28) Chandler, C. L.; List, B. *J. Am. Chem. Soc.* **2008**, *130*, 6737–6739.
- (29) Martin, S. F.; Dodge, J. A. *Tetrahedron Lett.* **1991**, *32*, 3017–3020.
- (30) Gomez-Vidal, J. A.; Forrester, M. T.; Silverman, R. B. *Org. Lett.* **2001**, *3*, 2477–2479.

- (31) Hunter, C. A.; Sanders, J. K. M. *J. Am. Chem. Soc.* **1990**, *112*, 5525–5534.
- (32) Salonen, L. M.; Ellermann, M.; Diederich, F. *Angew. Chem., Int. Ed.* **2011**, *50*, 4808–4842.
- (33) The 4*R*-acetoxypyrrolidine exhibited similar effects on ring pucker, although no effect on $K_{\text{trans/cis}}$ compared to 4*R*-hydroxypyrrolidine was observed: Jenkins, C. L.; McCloskey, A. I.; Guzei, I. A.; Eberhardt, E. S.; Raines, R. T. *Biopolymers* **2005**, *80*, 1–8.
- (34) Demange, L.; Ménez, A.; Dugave, C. *Tetrahedron Lett.* **1998**, *39*, 1169–1172.
- (35) Doi, M.; Nishi, Y.; Kiritoshi, N.; Iwata, T.; Nago, M.; Nakano, H.; Uchiyama, S.; Nakazawa, T.; Wakamiya, T.; Kobayashi, Y. *Tetrahedron* **2002**, *58*, 8453–8459.
- (36) Chorghade, M. S.; Mohapatra, D. K.; Sahoo, G.; Gurjar, M. K.; Mandlecha, M. V.; Bhoite, N.; Moghe, S.; Raines, R. T. *J. Fluorine Chem.* **2008**, *129*, 781–784.
- (37) The observation of different structures within the unit cell is potentially due to crystal-packing effects, in which the competition between π - π interactions and stereoelectronic effects leads to structural distortion. For an example of structures exhibiting the competition between crystal packing effects and stereoelectronic effects, see: Alabugin, I. V.; Manoharan, M.; Buck, M.; Clark, R. J. *THEOCHEM* **2007**, *813*, 21–27.
- (38) Briggs, A. J.; Glenn, R.; Jones, P. G.; Kirby, A. J.; Ramaswamy, P. *J. Am. Chem. Soc.* **1984**, *106*, 6200–6206.
- (39) Juaristi, E.; Cuevas, G. *Tetrahedron* **1992**, *48*, 5019–5087.
- (40) Alabugin, I. V.; Gilmore, K. M.; Peterson, P. W. *WIREs Comput. Mol. Sci.* **2011**, *1*, 109–141.
- (41) Parsons, S.; Flack, H. *Acta Crystallogr.* **2004**, *A60*, s61.
- (42) APEX2; Bruker-AXS Inc.: Madison, WI, 2005.
- (43) Sheldrick, G. M. *SHELX-2013*; University of Gottingen: Germany, 2013.